


FULL PAPER

Design optimization of an air atmospheric pressure plasma-jet device intended for medical use

Magalí Xaubet^{1,2}  | Jan-Simon Baudler³ | Torsten Gerling³ |
Leandro Giuliani^{1,2} | Fernando Minotti^{1,2} | Diana Grondona^{1,2} |
Thomas Von Woedtke³ | Klaus-Dieter Weltmann³

¹ Universidad de Buenos Aires, Facultad de Ciencias Exactas y Naturales, Departamento de Física, Pabellón 1, Ciudad Universitaria, 1428 Buenos Aires, Argentina

² CONICET - Universidad de Buenos Aires, Instituto de Física del Plasma (INFIP), Pabellón 1, Ciudad Universitaria, 1428 Buenos Aires, Argentina

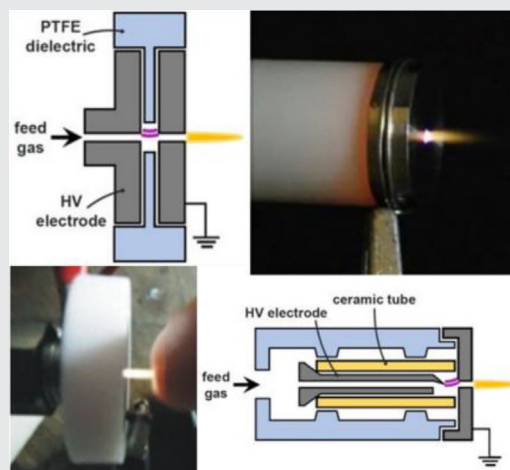
³ Leibniz Institute for Plasma Science and Technology (INP Greifswald e.V.), Felix Hausdorff-Straße 217489 Greifswald, Germany

Correspondence Magalí Xaubet, Departamento de Física, FCEyN, UBA and Instituto de Física del Plasma (INFIP), CONICET-UBA, Pabellón 1, Ciudad Universitaria, 1428 Buenos Aires, Argentina. Email: xmagali@df.uba.ar

Funding information

Ministry of Education, Science and Culture of the State of Mecklenburg-Vorpommern, Grant number: AU 15 001; Consejo Nacional de Investigaciones Científicas y Técnicas, Grant number: PIP 2013-2015 GI 11220120100453; Universidad de Buenos Aires, Grant number: UBACYT 2016 Mod I 20020150100096BA; Bundesministerium für Bildung und Forschung, Grant number: 13N13960; Seventh Framework Programme, Grant number: 316216; DAAD, Grant number: 57130097

The current and potential applications of atmospheric pressure plasmas in medicine generate an increasing need to develop safe and reliable plasma devices for patient treatment. This paper shows how the estimation of safety risks, the stability of the generated plasma, and the effectiveness in the aimed application can orientate the design process of a specific atmospheric pressure plasma device intended for clinical use. A promising plasma jet device operated with air is optimized, leading to a configuration with a more advanced design that reduces the temperature of the effluent, prevents the material degradation and improves the isolation of the high voltage components. The effects of the plasma jet treatment are investigated by chemical analysis of demineralized water and inactivation tests on *E. coli* cultures.



KEYWORDS

atmospheric pressure plasma jet, non-thermal plasma, plasma medicine, UV-VIS spectroscopy, VUV spectroscopy

1 | INTRODUCTION

Cold atmospheric pressure plasma devices for medical purposes became a widely researched field in the last decade.^[1–4] Investigations show that the direct application of non-thermal plasmas over tissue is promising in wound

healing and antiseptic therapies in dermatology.^[3,5–7] Potential uses in dentistry^[8,9] and oncology^[10–14] have also been in continuous study.

Based on comprehensive in vitro research using microorganisms and cell cultures three general biological plasma effects with relevance for medical applications have been

described repeatedly: (1) inactivation of a broad spectrum of microorganisms including multidrug resistant pathogens;^[15–17] (2) potential to stimulate cell proliferation and to promote tissue regeneration; and (3) ability to turn off mammalian cells and specially cancer cells by initialization of the programmed cell death (apoptosis).^[18]

In contrast to the extensive investigations of the biological effects of the cold plasma treatment and the chemical reactive species involved,^[19,20] the optimization of plasma sources for biological and medical applications remains to be brought to discussion. Related contributions focused on the temperature and the reproducibility of the plasma effluent^[21] and on the antimicrobial efficiency of the different plasma components (UV radiation and reactive species).^[22,23] Many plasma sources proposed for medical applications are derivatives of former research devices from physics laboratories that do not address usability, manufacturability, or safety requirements necessary for prospective medical devices. Nevertheless, the modifications in design and operation parameters to fit these needs can alter previous promising results in biological and medical tests in an unwanted way.

In this way, an example is presented in this work of how an actual experimental device, the INFIPjet, was modified following the considerations of some of the standards required for medical use. It is hoped that the presentation of the steps taken can be instructive and serve as a guide to be applied in similar situations.

1.1 | Requirements of plasma medical devices

The evaluation of potential risks based on safety standards is an essential procedure to request the certification of a medical product. As to this date there are however no international safety standards for plasma devices for medical purposes.

The risk estimation of plasma devices was discussed for applications in dermatology.^[24,25] These contributions were pursued by the publication of the German pre-standard DIN SPEC 91315 “General requirements for plasma sources in medicine”^[26] to provide general guidelines for the characterization of plasma sources in medicine. DIN SPEC 91315 test criteria include physical parameters like temperature, thermal output, leakage current, ultraviolet (UV) irradiance and toxic gas formation as well as estimations of antimicrobial effectivity and cytotoxicity.^[27] The aim of this pre-standard is not to define any threshold values or minimum performance requirements for medical plasma devices. It offers an option to obtain first and basic information about performance characteristics as well as effectiveness and safety of plasma devices suitable as therapeutic tools.

Despite the importance of obtaining comparable results in therapeutic applications, the process reproducibility in plasma medical devices was, to our knowledge, infrequently addressed. Process reproducibility can be defined in this

context as the maximum amount of fluctuations in time and in different ambient conditions tolerated for the clinical application. Being considered as the main biologically active components produced by plasma devices, the concentration of reactive species and the emitted radiation may act as direct process variables in a definition of reproducibility. Changes in the plasma regime, detected by fluctuations in the voltage-current waveforms or in the effluent temperature can be used as indirect parameters for stability quantifications.^[21]

In atmospheric pressure devices working in air environment the plasma forms from the ionization of the feeding gas admixed with the surrounding atmospheric air. It is an open question up to which amount the variations in the composition of the feed gas and changes of the environmental conditions may affect the reproducibility of the results. As observed for an argon plasma device,^[28] the humidity content in the feed gas alters significantly the chemical balance of the generated reactive species and the viability of HaCaT skin cells after plasma treatment. A considerable source of the feed gas humidity was noticed from the water desorption of the inner walls of the tubing connection.^[29] At the same time, dependence on the ambient humidity was found negligible along the examined range of about 0–40%rh, indicating reproducibility of results over a variety of ambient humidity conditions.^[28]

Reproducibility is also affected by the manufacture and the ageing of the device including the deterioration of parts in close contact with the plasma.^[30] Design parameters like the shape and the distance between electrodes can modify the characteristics of the gas discharge.^[31] For this reason, identical copies of complex devices tend to have manufacturing fluctuations and scattering of results. In the small scale production of a laboratory the use of simpler designs can achieve a better manufacturing accuracy.

A third main concern for the development of medical plasma sources is its effectiveness. The effectiveness of a particular plasma device is considered in this work as the quantification of the effects produced towards the aimed application. These effects need to be compared with other plasma devices and therapies in current use. Noteworthy is that due to regulations on human subjects research it is often inefficient or impossible to test the direct effect of devices under development. In vitro test models are in consequence a useful tool to evaluate and measure the biological effects of a plasma device^[32] and enable to later substantiate the role of the plasma treatment in in vivo experiments.^[33]

Among the in vitro examinations, the study of the chemical effects of the plasma treatment in liquid models including variations in the pH and in the concentrations of nitrite, nitrate and hydrogen peroxide, gives information about dissolved species that can serve as indicators for more complex oxygen and nitrogen chemistry as result of plasma-liquid interaction and can give some orientation about

expectable biological effects.^[32] Testing the inactivation efficiency using a set of standardized test microorganisms provides a comparable estimation of the biological effectiveness of plasma devices. This can be studied in simple humid models by means of inhibition zone tests in agar plates or by the treatment of microbial suspensions.^[27]

In this article, a specific plasma jet device operating in air at atmospheric pressure is optimized using physical methods based on DIN SPEC 91315 in order to evaluate both its performance characteristics and its safety. The degradation of the components and the stability of the observed effluent are considered as well in order to improve the design of the device. Additionally, the generation of reactive species is studied by emission spectroscopy and chemical changes produced on plasma treated water are evaluated. The biological effects produced by the exposition to the plasma effluent are studied by inactivation tests on *E. coli* cultures. Overall, the use of standardized methods attempts to quantify the performance of the optimized device to readily compare it with that of other plasma devices certified for medical purposes, like kINPen MED®.^[27]

2 | EXPERIMENTAL SECTION

The INFIPjet^[34] is an atmospheric pressure plasma jet device with an electrode geometry similar to that used in the devices of Hong^[35] and Kolb,^[36] but using a different voltage waveform and mechanism of current limitation. It is based on an air discharge without dielectric barrier formed in a gap between plane perforated electrodes (1 mm central perforation) separated by 1 mm. The discharge has the characteristics of a contracted glow with a relatively high voltage cathode layer.^[37] Electrodes are assembled by a dielectric of PTFE with a 3 mm central perforation (Figure 1a). The device is operated with 5 slm air flow from an air compressor and

powered by a 50 Hz oil burner shunted transformer (Magnetek, 15 kV) that limits the current amplitude to 30 mA.

The tests summarized later in this section were applied on INFIPjet to evaluate the safety and potential of the device intended for medical use. In response to the test results the design was optimized, leading to a more advanced design of the INFIPjet, called the Magiplas (Figure 1b). Magiplas device is formed by a frontal disc-shaped grounded electrode (15 mm outer diameter and 1 mm central perforation) and a rear high voltage needle electrode (2 mm outer and 1.5 mm inner diameter), both made of stainless steel and separated by 1 mm (Figure 1b). The tip of the needle electrode was made by cutting one end at an angle and lightly bending it towards the axis. Compared to INFIPjet, the high voltage electrode was reduced in size and covered by insulating materials to prevent electric risk. Instead of PTFE, a ceramic tube (3 mm inner diameter) was used to confine the gas flow.

Apart from the geometry modifications, the main changes in the Magiplas device are the flow rate and the electrical supply (see Figure 1). A total of 3.5 slm air flow is used to obtain a laminar effluent stream in the new configuration. To reduce the effluent temperature, Magiplas is supplied with a current amplitude of 20 mA and a 20% duty cycle burst modulation. For this purpose, electrical modifications (voltage reduction and 2 Hz pulse width modulation) were introduced at the input of the high voltage transformer as indicated in Figure 2.

The design modifications maintain however the main attribute of the original device: the generation of a direct discharge in air between concentric electrodes separated by 1 mm. A digital oscilloscope (Picoscope 5244B 200 MHz) set at 15 MS/s (megasamples per second) was employed to measure the voltage drop between electrodes using a high voltage probe (Tektronix P6015A 1000×), and the current determined from the voltage drop over a series resistor (100 Ω).

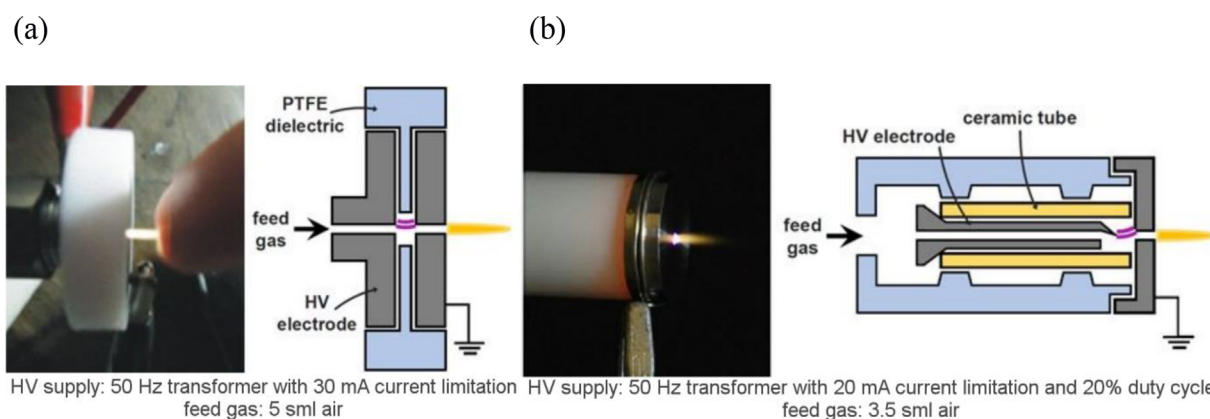


FIGURE 1 Photograph and cross-sectional scheme of (a) INFIPjet, the original version of the plasma device, and (b) Magiplas, the more advanced designed configuration. Powering and gas flow conditions are indicated for each device

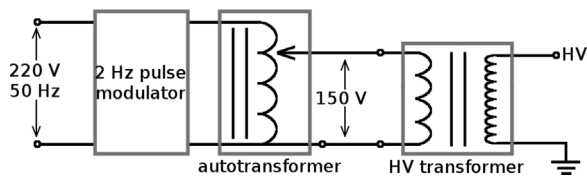


FIGURE 2 Powering circuit of Magiplas device showing the voltage reduction and the pulse width modulation introduced at the input of the high voltage transformer

The following measurements were applied to INFIPjet and Magiplas to evaluate and compare their potential for medical applications.

Effluent temperature and thermal output were measured as described in DIN SPEC 91315.^[26,27] The axial temperature of the effluent was measured with a fiber optic thermometer (Luxtron FOT STF) as function of the distance to the front electrode. The thermal output (P) was obtained calorimetrically using Equation (1),

$$P = mC \frac{dT}{dt} \quad (1)$$

For this determination, a copper plate target ($10 \times 10 \times 0.5 \text{ mm}^3$, mass $m = 312 \text{ mg}$, specific heat $C = 385 \text{ J g}^{-1} \text{ }^\circ\text{C}^{-1}$) was placed in front of the plasma effluent at different distances from the front electrode. The fiber optic thermometer was attached to the copper plate to register the variation in time of the temperature (dT/dt) due to the heat exchange with the effluent.

Measurements of patient leakage current were performed applying the effluent over a copper target ($40 \times 40 \times 1 \text{ mm}^3$) connected to a certified test device (Bender UNIMET 800ST) that contains a voltmeter and a low pass filter according to DIN EN 60601.^[38]

The spectral irradiance of the device in the 200–860 nm range was measured end on at 3 mm distance (estimated minimal working distance) using an irradiance calibrated spectrometer (Avantes–AvaSpec 3648) with an optical fiber (Avantes–UV600) and a cosine corrector (Avantes–CC UV/VIS).

Vacuum ultraviolet (VUV) spectroscopy is proposed in this work to monitor qualitatively the degradation of PTFE components present in the device using the 193 nm emission line of argon fluoride excimer (ArF). This line was already observed in the VUV spectrum of a plasma device operated with argon admixtures designed as part of a PTFE biopsy channel of an endoscope.^[30] The formation of ArF in that device was attributed to the recombination in the gas phase of fluoride atoms released from the PTFE tube walls.

The device emission was measured end on with a VUV apparatus as described in the paper of Foest et al.^[39] The main components of the setup are a VUV monochromator (ARC VM 505) with a 1200 lines/mm grating, a VUV

photomultiplier (Thorn/EMI 9635 QB) and a vacuum chamber with a pressure of $2 \cdot 10^{-4} \text{ Pa}$.

As this method requires the presence of argon in the ambient, the plasma devices were operated for this measurement with an argon flow of 3 slm. As a complement to VUV results, appreciable damage of PTFE components in the device was photographed.

The chemical composition of demineralized water was analyzed after treatment with the Magiplas device used in burst mode. A total of 5 ml of demineralized water were plasma treated. Immediately after the treatment, the pH was measured with a pH meter (TM40 Sensortechnik Meinsberg) and the concentrations of hydrogen peroxide (H_2O_2), nitrate (NO_3^-), and nitrite (NO_2^-) were determined photometrically as described by Oehmigen et al.^[40] using, respectively, titanil sulfate and commercial test kits (1.09713 and 1.14776 Spectroquant Merck). To measure the absorbance, a spectrophotometer (VWR UV-3100PC) was used. Additionally, the biological activity of the Magiplas used in burst mode was studied using *Escherichia coli* K-12 DSM 11250/NCTC 10538 in two microbiological test systems: by inhibition zone tests on wet solid nutrient media (agar) and in bacteria suspensions in physiological saline (0.85%NaCl[w/v]) as proposed in DIN SPEC 91315.^[26,27]

For inhibition zone assay, overnight precultures of *E. coli* were centrifuged (5000 g) and the pellets were resuspended in physiological saline to get a stock suspension with a concentration of 10^5 colony forming units per milliliter (CFU/ml). Agar plates (diameter 90 mm) filled with tryptic soy agar (Merck) were inoculated with 100 ml of the bacteria suspension. Afterwards, localized spot-like plasma treatments were carried out on the inoculated agar plates. After overnight incubation at 37°C the diameter of the inhibition zone was measured.

For inactivation test in bacteria suspension, 5 ml of the *E. coli* microbial suspension (initial concentration of 10^5 CFU/ml) were plasma treated. Suspensions were afterwards plated on agar with a spiral plater (IUL instruments Eddy jet 2). After overnight incubation at 37°C , CFU/ml was determined.

For all these tests, the plasma device was placed centrally, with the visible tip of the effluent reaching the liquid or medium surface (equivalent to a distance of 6 mm). One to five minutes treatment times were tested, performing six repetitions for statistical analysis. The evaporation of water was estimated around $180 \mu\text{l}$ for 5 ml of liquid at the maximum treatment time (around 4% of the treated volume) and was not considered in the analysis of results.

3 | RESULTS AND DISCUSSION

3.1 | Electrical signals

The similarity between INFIPjet and Magiplas can be observed in the electrical signals (Figure 3a and 3b) obtained

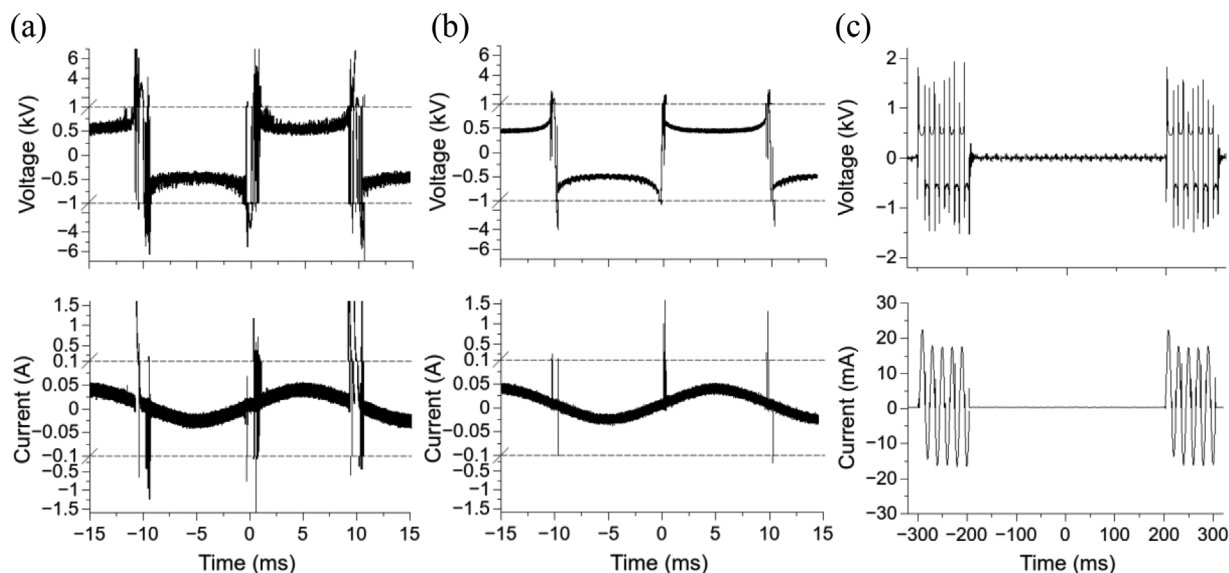


FIGURE 3 Voltage and current waveforms of INFIPjet (a) and Magiplas (b), under the same powering conditions (30 mA current limitation). Vertical axes are cut and rescaled to show both the 50 Hz continuum signal and the spike height. (c) Voltage and current waveforms of Magiplas in burst mode (20% duty cycle burst modulation with a 2 Hz modulation signal)-voltage and current spikes are less visible in (c) due to the different horizontal scale

at the same powering conditions (30 mA current limitation). Comparable signals are registered, showing a current with sinusoidal profile of 30 mA amplitude and voltage around 500 V that decreases as the current increases. This relatively low voltage is due to the high conductivity of the plasma channel that develops after a breakdown phase. The breakdown phase appears at the beginning of each half cycle when the applied voltage reaches values around 5 kV for INFIPjet and 2 kV for Magiplas and is observed in the electrical signals as current and voltage spikes (of about 100 μ s duration) corresponding to micro-arcs interrupted by the high inductance behavior of the power source before the more stable discharge is established.^[37,41,42] The shape modification of the rear electrode to a sharp needle intensifies the electric field on the central axis producing a decrease in the breakdown potential that can explain the reduction by about half in the number of spikes of Magiplas.

In burst mode conditions, Magiplas is powered with a 20% burst modulation of 2 Hz. The resulting voltage and current waveforms are depicted in Figure 3c.

3.2 | Safety parameters

The effluent temperature of INFIPjet (see Figure 4a) exceeds the regulated 37 °C maximum temperature for application on human body,^[38] motivating the current reduction and burst modulation of Magiplas, which brought the temperatures around 35 °C. In Figure 4b, the effluent thermal output including its reduction in the new design is additionally shown.

For a better comparison with INFIPjet, measurements corresponding to Magiplas operation in continuum mode are

also presented, showing simultaneously increased effluent temperatures and reduced thermal output (Figure 4). The reduced air flow in Magiplas can explain both observations, as the feed gas has a cooling effect over the device, but it is as well a means of heat exchange with the treated target.

At working distances as close as 1 mm from the front electrode, the leakage current of INFIPjet and Magiplas was below the 1 μ A detection limit of the measuring device and at the same time, below the safety limitation of 100 μ A for normal operating conditions.^[38] This result is possibly related to the small size of the perforation of the grounded electrode, through which the jet emerges, as compared with the Debye length of the emerging tenuous plasma.

Spectral irradiance of INFIPjet and Magiplas is shown on Figure 5. The emission spectrum presents bands of NO gamma system, N₂ first and second positive system, N₂⁺ first negative system and O lines at 777.4 and 844.6 nm.^[43,44] As the type of discharge and the operating gas were preserved in the design optimization, the excited species present are similar in both versions of the device.

Irradiance between 200 and 400 nm was calculated from the spectral irradiance integral, using the weight factors given by the International Commission on Non-Ionizing Radiation Protection (ICNIRP)^[45] to determine the suggested skin exposure limit to UV broadband sources to minimize long term risk. Obtained values were 2.95 ± 0.05 , 2.99 ± 0.08 , and $0.30 \pm 0.05 \mu\text{W cm}^{-2}$, respectively, for INFIPjet, Magiplas in continuum mode and Magiplas with burst operation. The improved radial confinement of the discharge channel in Magiplas compensates for the use of a lower current, leading to the similar irradiance values of INFIPjet and Magiplas in

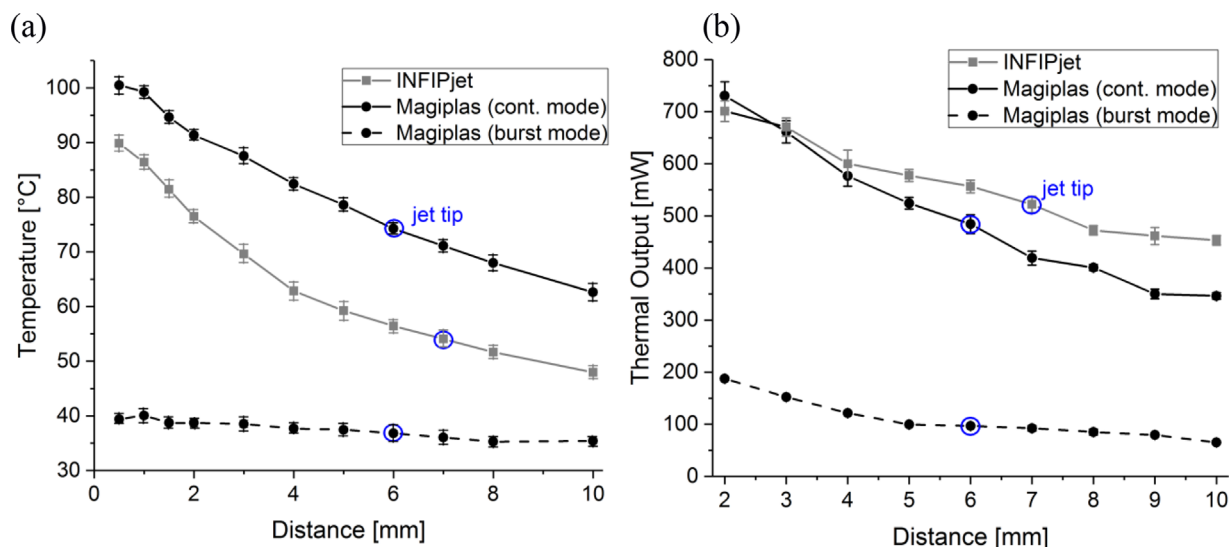


FIGURE 4 Temperature (a) and thermal output (b) profile of the effluent of INFIPjet and Magiplas with continuous and burst operation. Distance corresponding to jet tip (visible end of the effluent) is marked in blue (average taken over three measurements)

continuum operation. The burst operation reduces the irradiance of the Magiplas device to about a tenth of that in continuum operation, bringing it close to the detection limit of the experimental setup. According to the guidelines of human daily UV exposure of ICNIRP,^[45] the measured irradiance values limit the daily steady exposure to 15 min for INFIPjet and Magiplas in continuum mode, and can be extended up to 2.7 h in burst mode.

3.3 | Observations related to reproducibility

Intermittence of the visible effluent was observed on INFIPjet due to fluctuations in the position of the discharge channel around the central electrode perforation. The use of a sharp-edged rear electrode in Magiplas intensifies the electric field

on the central axis, improving the electrical lateral confinement of the gas discharge and producing as well a decrease in the breakdown potential. As a result, a stable and intense effluent was obtained with Magiplas despite the use of a lower operating current.

Over-prolonged continuum use of INFIPjet device (8 h) revealed that the PTFE insulator was being degraded in the proximity of the discharge channel (Figure 6). This observation compromised the durability of the device and the reproducibility of the discharge shown in a marked increase in the noise of the electrical signal. Also, this behavior may affect the safety of the device due to the possible formation of toxic fluorine by-products.

In Magiplas design, PTFE surrounding the discharge channel was avoided and the gas flow was laterally confined by a ceramic tube. Degraded dielectric material was not further observed in the new device. Only the inner electrode

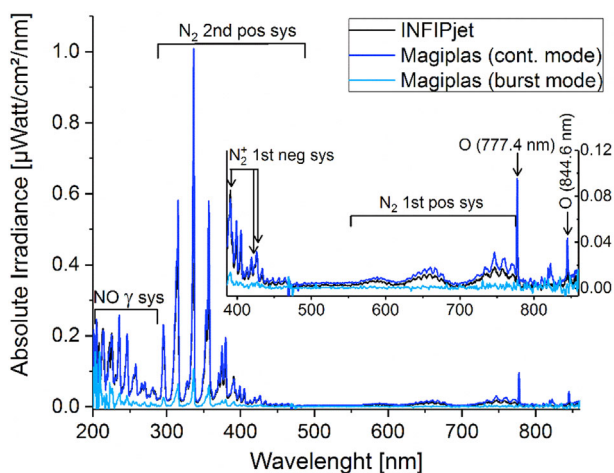


FIGURE 5 Spectral irradiance of INFIPjet and Magiplas with continuous and burst operation

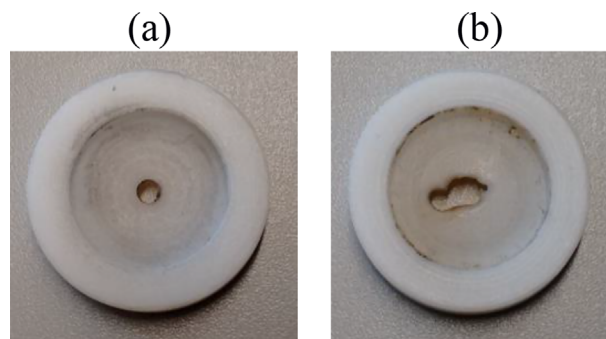


FIGURE 6 Pictures of the PTFE insulator (a) before and (b) after over-prolonged continuum operation (8 h) of INFIPjet, showing degradation in regions close to the discharge channel

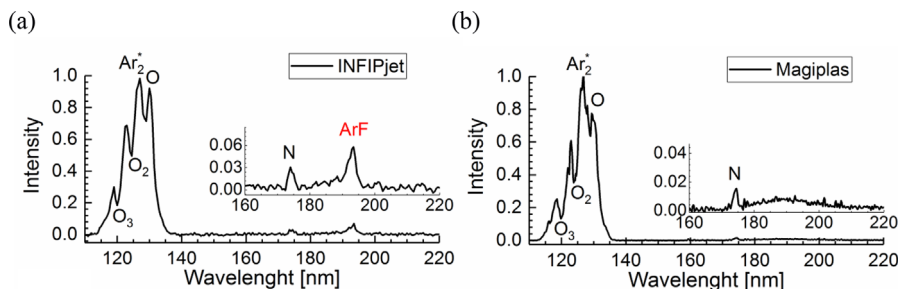


FIGURE 7 VUV emission spectrum of (a) INFIPjet and (b) Magiplas in continuum operation using 3 slm argon as feed gas

presented signals of degradation after about 15 days of use in cycles of 2 h continuous operation each day.

Figure 7 shows the VUV emission spectrum using argon as a feed gas. The spectrum is formed by the broad 2nd continuum of the argon excimer Ar_2^* centered at 126 nm, a N line at 174 nm and an O line at 130 nm.^[46] The Ar_2^* continuum band is overlapped with absorption lines, attributed to the presence of O_3 (121 nm) and O_2 (125 nm) as in the paper of Polak et al.^[30] Consistent with the PTFE degradation observed only on INFIPjet device, ArF 193 nm line is absent in Magiplas emission spectrum.

3.4 | In vitro performance

Results of the chemical analysis of demineralized water treated with the Magiplas plasma device are presented in Figure 8a. NO_2^- concentration increased linearly with treatment time, up to 8 mg l^{-1} for 5 min treatments. At the same time, acidification of the medium was registered, reaching 3.7 pH values for the longest treatment time. H_2O_2 and NO_3^- formation was not observed for any treatment time, considering the respective method detection limits, of 0.05 and 0.07 mg l^{-1} .

Acidification is relevant against bacterial proliferation, as most skin pathogenic bacteria growth is inhibited below pH 6.^[47] As discussed by Oehmigen et al.,^[40] the acidification can be attributed to the formation of nitrous acid (HNO_2) from

NO via NO_2 . If acidification occurs mainly due to the dissolution of HNO_2 , it is to be expected that the concentration of H^+ and NO_2^- is the same for equal treatment times. In this sense, Figure 8b shows a correlation between the molar concentration of NO_2^- , calculated considering its molar mass of 46 g mol^{-1} , and the molar concentration of H^+ deduced from the definition of pH.

Finally, the absence of H_2O_2 may be related to the lack of OH radicals in the gas phase indicated by the absence of OH lines in the emission spectrum (Figure 5). In argon plasma jets, where argon metastables react with water molecules forming gaseous OH radicals,^[48] it is considered that a major source of H_2O_2 in the liquid phase is the diffusion of gaseous H_2O_2 formed by OH radical recombination.^[49]

The registered inhibition zones (Figures 9a and 9c) are comparable in size to the ones produced by argon plasma jet devices for local treatment^[5,24,27,50–52] at similar treatment times. Meanwhile, the CFU count of the treated microbial suspensions (Figure 9b) shows that Magiplas effluent causes a minor bulk inactivation on *E. coli* as the CFU/ml decreases to about half of the starting value for treatment times up to 5 min. It is worth to point out that the treated suspension volume was relatively large (5 ml) leading to a smaller inhibition effect than other plasma devices that report reduction values up to log 3 after 5 min treatments using suspension volumes of tens or hundreds of microliters.^[22,53,54] Dependence of the

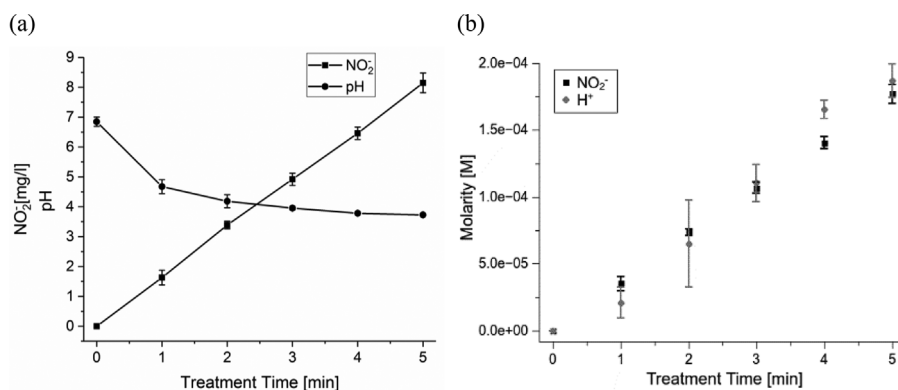


FIGURE 8 (a) pH values and nitrite concentration of demineralized water for different treatment times performed by Magiplas in burst mode (average taken over six measurements). (b) Calculated molarities

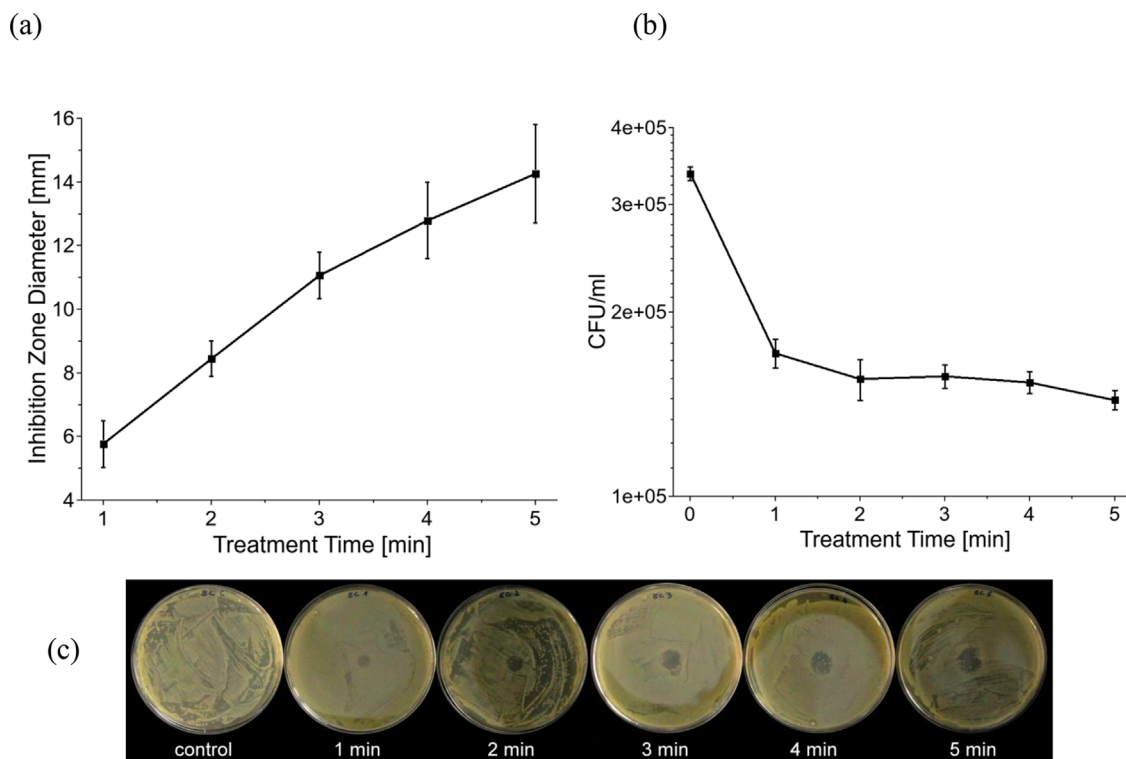


FIGURE 9 (a) Inhibition zone diameter and (b) CFU/ml for different treatment times performed by Magiplas in burst mode (average taken over six measurements). (c) Pictures of the inhibition zones obtained after treating the center of the petri dishes

inactivation performance on the treated volume was studied for a 1.5–10 ml suspension volume range using an air surface DBD^[40] finding a less significant inactivation as the volume increases for different microbial strains.

These results appear to indicate, on the one hand, the importance of using standardized methods for comparing the performance of plasma treatments and also, as suggested by Mann et al.,^[27] the need of reviewing and improving the sensitivity of the method proposed in DIN SPEC 91315 for studying bulk inactivation.

3.5 | General remarks of magiplas device and comparison with a medically certified plasma device

The results obtained in this work for Magiplas can be readily compared with the ones measured for kINPen MED[®]^[27] as the same methods based on DIN SPEC 91315 were used on both devices. This comparison gives also relevant information in terms of risk estimation as the kINPen MED[®] is already certified as medical device. As presented in Table 1, it

TABLE 1 Comparison between results obtained with Magiplas and kINPen MED[®].^[27] (jet tip means the visible end of the effluent)

| | Magiplas | kINPen MED [®] |
|--|--|--|
| Operating conditions | Air 3.5 slm needle to plane electrodes 50 Hz direct discharge 20% burst modulation | Argon 5 slm rod to ring electrodes 1 MHz DBD discharge 50% burst modulation |
| Effluent temperature at jet tip (°C) | 36–38 | 35–38 |
| Thermal output at jet tip (mW) | 90–100 | 145–160 |
| Leakage current at jet tip (μA) | <1 | 20–40 |
| Irradiance (μW cm ⁻²) ^{a)} | 0.30 ± 0.05 [200–400 nm] ^{a)} | 10–30 [280–380 nm] ^{a)} |
| Optical emission spectroscopy | NO, N ₂ ⁺ , O | OH, N ₂ ⁺ , O |
| Chemical analysis ^{b)} | pH: 4, NO ₂ ⁻ | pH: 6, H ₂ O ₂ , NO ₃ ⁻ , NO ₂ ⁻ |
| Antimicrobial assays on <i>E. coli</i> ^{b)} | Inactivation: log 0.5 14 mm inhibition zone | Inactivation: log 0.1 18 mm inhibition zone |

^{a)}Using ICNIRP weight factors.^[45] Note that irradiance was integrated from different wavelength ranges.

^{b)}Results corresponding to a 5 min treatment.

is notable that despite the differences in the operating conditions (gas type, electrode geometry, powering frequency, and discharge type) both devices achieve similar safety risk parameters.

As an outcome of the optimization process, Magiplas exhibited an effluent temperature suitable for patient therapy, and a very low leakage current, at least one order of magnitude below the typical values of KINPen MED® and two orders of magnitude below the IEC 60601-1 safety limit.^[38] These minimal values may be of interest for the treatment of patients with a low sensitivity threshold to electric current.

Magiplas showed a plasma chemistry dominated by nitrogen. O and NO reactive species were found in the gaseous phase. Consequent with these results, inactivation of *E. coli* was detected by inhibition zone tests. Although KINPen MED® has a different plasma chemistry based on oxygen species, the antimicrobial effects of both devices were found of similar magnitude. As it was stated above, the large volume used to study the bulk plasma treatment may explain the negligible log reduction measured for both devices.

4 | CONCLUSION

In this work, the design optimization of plasma devices intended for medical use and in an early development stage was discussed, based on the concepts of safety (effluent temperature, thermal output, leakage current, and UV radiation), reproducibility (stability of the electrical signals and of the visible effluent, lack of degradation of components) and effectiveness.

The plasma source under study was an air jet device without dielectric barrier between the electrodes. Effluent temperature and stability as well as material degradation were the main aspects improved in the redesign, while preserving simultaneously the type of electric discharge, the operating gas and the generated reactive species. A better isolation of the HV components was also carried out, leading to an easy to handle and economic device that is fed with pressurized air and powered by a shunted transformer.

A qualitative method for the study of PTFE damage was proposed, showing results consistent with the material degradation observed after over-prolonged operation. These measurements point out that the interaction between plasma and device components can affect the biocompatibility of certified medical materials and lead to the formation of toxic substances.

As the device produces UV radiation, reactive oxygen and nitrogen species, future experiments may clarify if any component holds the main contribution to the biological effects.

Concerning the potential of use in clinical therapy and the requirement of a medical certification, the risk estimation of side effects must still be complemented with in vitro

experiments of cytotoxicity and mutagenicity on eukaryotic cells. To go further in the study of the medical potential of the device a precise application needs to be defined such as tissue growth stimulation or decontamination. It is also relevant to study the penetration depth of the desirable and the undesirable effects in tissue, testing them initially over suitable models.^[55]

ACKNOWLEDGMENTS

The authors MX, LG, FM, and DG would like to acknowledge the funding from CONICET (PIP GI11220120100453) and from the University of Buenos Aires (UBACYT 2016 Mod I20020150100096BA). JSB, TG, TvW, and KDW are grateful for the funds received from the German Ministry of Education and Research (BMBF 13N13960) and from the Ministry of Education, Science, and Culture of the State of Mecklenburg-Vorpommern (AU 15 001). The work has received funding from the European Union Seventh Framework Program (FP7/2007-2013 316216) and from DAAD (Short-Term Grant 57130097).

ORCID

Magalí Xaubet  <http://orcid.org/0000-0002-2340-6965>

REFERENCES

- [1] G. Fridman, G. Friedman, A. Gutsol, A. B. Shekhter, V. N. Vasilets, A. Fridman, *Plasma Process. Polym.* **2008**, *5*, 503.
- [2] M. G. Kong, G. Kroesen, G. Morfill, T. Nosenko, T. Shimizu, J. Van Dijk, J. L. Zimmermann, *New. J. Phys.* **2009**, *11*, 115012.
- [3] T. von Woedtke, H. R. Metelmann, K. D. Weltmann, *Contrib. Plasma Phys.* **2004**, *54*, 104.
- [4] K.-D. Weltmann, T. von Woedtke, *Plasma Phys. Contr. Fusion* **2017**, *59*, 014031.
- [5] G. Daeschlein, S. Scholz, A. Arnold, S. Von Podewils, H. Haase, S. Emmert, T. von Woedtke, K. D. Weltmann, M. Jünger M, *Plasma Process Polym.* **2012**, *9*, 380.
- [6] G. Isbary, J. L. Zimmermann, T. Shimizu, Y. F. Li, G. E. Morfill, H. M. Thomas, B. Steffes, J. Heinlin, S. Karrer, W. Stolz W, *Clin Plasma Med.* **2013**, *1*, 19.
- [7] S. Emmert, F. Brehmer, H. Hänßle, A. Helmke, N. Mertens, R. Ahmed, D. Simon, D. Wandke, W. Maus-Friedrichs, G. Däschlein, M. P. Schön Wolfgang Viöl, *Clin. Plasma Med.* **2013**, *1*, 24.
- [8] D. S. Singh, D. R. Chandra, D. S. Tripathi, D. H. Rahman, D. P. Tripathi, D. A. Jain, D. P. Gupta, *IOSR J. Dent. Med. Sci.* **2014**, *13*, 06.
- [9] E. Simoncelli, D. Barbieri, R. Laurita, A. Liguori, A. Stancampiano, L. Viola, R. Tonini, M. Gherardi, V. Colombo, *Clin. Plasma Med.* **2015**, *3*, 77.
- [10] J. Schlegel, J. Körtzer, V. Boxhammer, *Clin. Plasma Med.* **2013**, *1*, 2.
- [11] E. Robert, M. Vandamme, L. Brullé, S. Lerondel, A. Le Pape, V. Sarron, D. Riès, T. Darny, S. Dozias, G. Collet, C. Kieda, J. M. Pouvesle, *Clin. Plasma Med.* **2013**, *1*, 8.

- [12] H. Kajiyama, K. Nakamura, F. Utsumi, H. Tanaka, M. Hori, F. Kikkawa, *Jpn. J. Appl. Phys.* **2014**, *53*, 05FA05.
- [13] V. Miller, A. Lin, A. Fridman, *Plasma Chem. Plasma Process.* **2016**, *36*, 259.
- [14] A. M. Hirst, F. M. Frame, M. Arya, N. J. Maitland, D. O'Connell, *Tumor Biol.* **2016**, *37*, 7021.
- [15] S. A. Ermolaeva, A. F. Varfolomeev, M. Y. Chernukha, D. S. Yurov, M. M. Vasiliev, A. A. Kaminskaya, M. M. Moisenovich, J. M. Romanova, A. N. Murashev, I. I. Selezneva, T. Shimizu, E. V. Sysolyatina, I. A. Shaginyan, O. F. Petrov, E. I. Mayevsky, V. E. Fortov, G. E. Morfill, B. S. Naroditsky, A. L. Gintsburg, *J. Med. Microbiol.* **2011**, *60*, 75.
- [16] E. Kvam, B. Davis, F. Mondello, A. L. Garner, *Antimicrob. Agents Chemother.* **2012**, *56*, 2028.
- [17] N. O'Connor, O. Cahill, S. Daniels, S. Galvin, H. Humphreys, *J. Hosp. Infect.* **2014**, *88*, 59.
- [18] T. von Woedtke, S. Reuter, K. Masur, K.-D. Weltmann, *Phys. Rep.* **2013**, *530*, 291.
- [19] D. B. Graves, *J. Phys. D Appl. Phys.* **2012**, *45*, 263001.
- [20] X. Lu, G. V. Naidis, M. Laroussi, S. Reuter, D. B. Graves, K. Ostrikov, *Phys. Rep.* **2016**, *630*, 1.
- [21] J. Golda, J. Held, B. Redeker, M. Konkowski, P. Beijer, A. Sobota, G. Kroesen, N. St. J. Braithwaite, S. Reuter, M. M. Turner, T. Gans, D. O'Connell, V. Schulz-von der Gathen, *J. Phys. D Appl. Phys.* **2016**, *49*, 84003.
- [22] T. Nosenko, T. Shimizu, G. E. Morfill, *New J. Phys.* **2009**, *11*, 115013.
- [23] J.-W. Lackmann, S. Schneider, E. Edengeiser, F. Jarzina, S. Brinckmann, E. Steinborn, M. Havenith, J. Benedikt, J. E. Bandow, *J. Royal Soc Interface* **2013**, *10*, 20130591.
- [24] K.-D. Weltmann, E. Kindel, R. Brandenburg, C. Meyer, R. Bussiahn, C. Wilke, T. von Woedtke, *Contrib. Plasma Phys.* **2009**, *49*, 631.
- [25] R. Tiede, J. Hirschberg, G. Daeschlein, T. von Woedtke, W. Vioel, S. Emmert, *Contrib. Plasma Phys.* **2014**, *54*, 118.
- [26] DIN-SPEC 91315: General requirements for medical plasma sources (in German), Beuth-Verlag, Berlin, Germany **2014**.
- [27] M. S. Mann, R. Tiede, K. Gavenis, G. Daeschlein, R. Bussiahn, K.-D. Weltmann, S. Emmert, T. von Woedtke, R. Ahmed, *Clin. Plasma Med.* **2016**, *4*, 35.
- [28] S. Reuter, J. Winter, S. Iseni, A. Schmidt-Bleker, M. Dünnbier, K. Masur, K. Wende, K.-D. Weltmann, *IEEE Trans. Plasma Sci.* **2015**, *34*, 3185.
- [29] J. Winter, K. Wende, K. Masur, S. Iseni, M. Dünnbier, M. U. Hammer, H. Tresp, K.-D. Weltmann, S. Reuter, *J. Phys. D Appl. Phys.* **2013**, *46*, 295401.
- [30] M. Polak, J. Winter, U. Schnabel, J. Ehlbeck, K.-D. Weltmann, *Plasma Process. Polym.* **2012**, *9*, 67.
- [31] X. Hao, A. M. Mattson, C. M. Edelblute, M. A. Malik, L. C. Heller, J. F. Kolb, *Plasma Process. Polym.* **2014**, *11*, 1044.
- [32] K.-D. Weltmann, T. von Woedtke, *Eur. Phys. J. Appl. Phys.* **2011**, *55*, 13807.
- [33] G. Daeschlein, T. von Woedtke, E. Kindel, R. Brandenburg, K.-D. Weltmann, M. Ju, *Plasma Process. Polym.* **2010**, *7*, 224.
- [34] L. Giuliani, M. Xaubet, D. Grondona, F. Minotti, H. Kelly H, *Phys Plasmas.* **2013**, *20*, 063505.
- [35] Y. C. Hong, H. S. Uhm, *Phys. Plasmas.* **2007**, *14*, 053503.
- [36] J. F. Kolb, A. A. H. Mohamed, R. O. Price, R. J. Swanson, A. Bowman, R. L. Chiavarini, M. Stacey, K. H. Schoenbach, *Appl. Phys. Lett.* **2008**, *92*, 241501.
- [37] M. Xaubet, L. Giuliani, D. Grondona, F. Minotti, *Phys. Plasmas* **2017**, *24*, 013502.
- [38] DIN EN 60601-1-10:2016-04 Medical electrical equipment – Part 1: General requirements for basic safety and essential performance, Beuth- Verlag, Berlin, Germany 2016.
- [39] R. Foest, E. Kindel, H. Lange, A. Ohl, M. Stieber, K.-D. Weltmann, *Contrib. Plasma Phys.* **2007**, *47*, 119.
- [40] K. Oehmigen, M. Hähnel, R. Brandenburg, C. Wilke, K.-D. Weltmann, T. von Woedtke, *Plasma Process. Polym.* **2010**, *7*, 250.
- [41] M. Lu, X. Wang, Y. Pu, Z. Guan, *Plasma Sci. Technol.* **2008**, *10*, 185.
- [42] X. Li, X. Tao, Y. Yin, *IEEE Trans. Plasma Sci.* **2009**, *37*, 759.
- [43] R. W. B. Pearse, A. G. Gaydon, *The Identification of Molecular Spectra*, Whitefriars Press, London, UK **1963**.
- [44] A. Kramida, Y. Ralchenko, J. Reader, NIST ASD Team, NIST Atomic Spectra Database (version 5.5.1) <http://physics.nist.gov/asd>. (accessed on October 2017).
- [45] International Commission on Non-Ionizing Radiation Protection. *Health Phys.* **2004**, *87*, 171.
- [46] J. A. Samson, *Techniques of Vacuum Ultraviolet Spectroscopy*, John Wiley & Sons, New York, USA **1967**.
- [47] A. Helmke, D. Hoffmeister, N. Mertens, S. Emmert, J. Schuette, W. Vioel, *New J. Phys.* **2009**, *11*, 115025.
- [48] A. Schmidt-Bleker, J. Winter, S. Iseni, M. Dünnbier, K.-D. Weltmann, S. Reuter, *J. Phys. D. Appl. Phys.* **2014**, *47*, 145201.
- [49] J. Winter, H. Tresp, M. U. Hammer, S. Iseni, S. Kupsch, A. Schmidt-Bleker, K. Wende, M. Dünnbier, K. Masur, K.-D. Weltmann, S. Reuter, *J. Phys. D. Appl. Phys.* **2014**, *47*, 285401.
- [50] M. J. Kirkpatrick, B. Dodet, E. Odic, *Int. J. Plasma Environ. Sci. Technol.* **2007**, *1*, 96.
- [51] T. Shimizu, B. Steffes, R. Pompl, F. Jamitzky, W. Bunk, K. Ramrath, M. Georgi, W. Stolz, H.-U. Schmidt, T. Urayama, S. Fujii, G. E. Morfill, *Plasma Process. Polym.* **2008**, *5*, 577.
- [52] G. Daeschlein, M. Napp, S. von Podewils, S. Lutze, S. Emmert, A. Lange, I. Klare, H. Haase, D. Gümbel, T. von Woedtke, M. Jünger, *Plasma Process. Polym.* **2014**, *11*, 175.
- [53] R. E. J. Sladek, E. Stoffels, R. Walraven, P. J. A. Tielbeek, R. A. Koolhoven, *IEEE Trans. Plasma Sci.* **2004**, *32*, 1540.
- [54] P. Lukes, E. Dolezalova, I. Sirova, M. Clupek, *Plasma Sources Sci. Technol.* **2014**, *23*, 015019.
- [55] S. Bekeschus, A. Schmidt, K.-D. Weltmann, T. von Woedtke, *Clin. Plasma Med.* **2016**, *4*, 19.

How to cite this article: Xaubet M, Baudler J-S, Gerling T, et al. Design optimization of an air atmospheric pressure plasma-jet device intended for medical use. *Plasma Process Polym.* 2018;e1700211, <https://doi.org/10.1002/ppap.201700211>